

Effect of Hydrogen-Bond Strength on the Vibrational Relaxation of Interfacial Water

Ali Eftekhari-Bafrooei and Eric Borguet*

Department of Chemistry, Temple University, Philadelphia, Pennsylvania 19122

Received September 11, 2009; E-mail: eborguet@temple.edu

Abstract: Time-resolved sum frequency generation (tr-SFG) reveals that the vibrational energy relaxation rate of O–H stretching of dilute HDO in D₂O at the silica interface is markedly different from that of bulk water. As compared to the bulk liquid, the vibrational lifetime (T_1) of HDO is shorter at the charged surface than in the bulk, but longer at the neutral surface. The vibrational decoupling of the O–H of the HDO species leads to the observation of a frequency-dependent T_1 of the O–H stretch, which is shorter at the red than the blue side of the hydrogen-bonded OH spectral region. This correlates with the red-shift of the SFG spectra with increasing surface charge and is consistent with a theoretical model that relates the vibrational lifetime to the strength of the hydrogen-bond network.

1. Introduction

Predicting and engineering chemical and biological processes requires a deep understanding of the pathways and mechanisms of vibrational energy flow within the system. A vital step in chemical reactions is the accumulation of internal energy in the reactant molecules, which can lead, for example, to the breaking of old bonds and the formation of new bonds. The study of chemical reactions is therefore inevitably connected with vibrational energy relaxation processes.^{1,2} In mode selective chemistry, where one would like to break a specific bond, it is important to know how fast and to which modes the excess energy of an initially excited state redistributes.³ For molecules in the gas phase, the study, and therefore the control, of energy relaxation is less complicated; there is essentially no intermolecular relaxation. In the condensed phase, however, where a larger number of modes compete to accept the excess energy, it is more critical to know the mechanisms of relaxation processes.^{1,3}

Water is the solvent for a large body of chemical reactions that take place in chemical and biological systems. Of particular importance is the highly directional hydrogen-bond network, whose structure and dynamics dictate the unique chemical and physical properties of liquid water. The vibrational spectroscopy of the O–H stretching region is an excellent probe of the hydrogen-bond network and, to a large extent, is well understood in the bulk phase. An array of experiments and theories have revealed the pathways and time scales associated with different aspects of the vibrational dynamics of bulk water.⁴ However, our understanding of water molecules at surfaces and interfaces has not reached the level of bulk. Given the fact that the properties of interfacial water are essential for a variety of disciplines including biology (e.g., protein folding and membrane functions), atmospheric chemistry (e.g., pollution), and

electrochemistry (e.g., wetting and corrosion), it is of great interest to study the structure and dynamics of interfacial water and to learn how they might differ from the bulk.

This goal, however, has been hindered by the lack of appropriate experimental tools with high surface specificity and sensitivity. Second-order nonlinear spectroscopic methods, such as second-harmonic generation (SHG) and sum-frequency generation (SFG), offer great surface specificity and have become popular techniques for the study of interfaces in the past two decades.⁵ These techniques have reached the stage where they can routinely be applied for the investigation of the structure of interfacial water at the molecular level.^{5–7} SFG can be conducted either in the frequency (static SFG) or in the time domain (time-resolved SFG). The frequency domain SFG vibrational spectrum provides information on the structure, orientation, concentration, and chemical signature of the surface species. Time domain SFG probes the rates and pathways of vibrational energy transfer and vibrational dephasing. While the structure of water at various interfaces has been investigated via static SFG spectroscopy by numerous research groups,^{5–7} information on the interfacial vibrational dynamics is limited.^{8–11}

The coupling of vibrational modes in H₂O implies that the O–H stretching vibration is not localized on a single O–H bond, resulting in rapid spectral diffusion and fast intermolecular energy transfer.^{12–14} To decouple O–H groups within an individual water molecule, on the one hand, and between

(1) Nitzan, A. *Nature* **1999**, *402*, 472+.

(2) Barbara, P. F.; Walker, G. C.; Smith, T. P. *Science* **1992**, *256*, 975–981.

(3) Tully, J. C. *Science* **2006**, *312*, 1004–1005.

(4) Nibbering, E. T. J.; Elsaesser, T. *Chem. Rev.* **2004**, *104*, 1887–1914.

(5) Shen, Y. R.; Ostroverkhov, V. *Chem. Rev.* **2006**, *106*, 1140–1154.

(6) Richmond, G. L. *Chem. Rev.* **2002**, *102*, 2693–2724.

(7) Gopalakrishnan, S.; Liu, D. F.; Allen, H. C.; Kuo, M.; Shultz, M. J. *Chem. Rev.* **2006**, *106*, 1155–1175.

(8) Smits, M.; Ghosh, A.; Sterrer, M.; Muller, M.; Bonn, M. *Phys. Rev. Lett.* **2007**, *98*, 098302.

(9) Smits, M.; Ghosh, A.; Bredenbeck, J.; Yamamoto, S.; Muller, M.; Bonn, M. *New J. Phys.* **2007**, *9*, 390.

(10) McGuire, J. A.; Shen, Y. R. *Science* **2006**, *313*, 1945–1948.

(11) Eftekhari-Bafrooei, A.; Borguet, E. *J. Am. Chem. Soc.* **2009**, *131*, 12034–12035.

(12) Woutersen, S.; Bakker, H. J. *Nature* **1999**, *402*, 507–509.

(13) Deak, J. C.; Rhea, S. T.; Iwaki, L. K.; Dlott, D. D. *J. Phys. Chem. A* **2000**, *104*, 4866–4875.

surrounding water molecules, on the other, steady-state and ultrafast spectroscopy of bulk water^{15–17} as well as the steady-state SFG spectroscopy, but not the dynamics, of interfacial water have focused on the O–H (O–D) stretching vibration of dilute HDO in D₂O (H₂O).^{18–20} The rate of inter- and intramolecular energy transfer from excited OH modes of dilute HDO in D₂O decreases as compared to pure H₂O because the frequency of the O–D stretching mode is far below that of the O–H mode. Furthermore, decoupling the O–H and O–D oscillators within a single HDO species reduces intramolecular energy transfer so that information on the intrinsic lifetime of the decoupled O–H vibration can be obtained. Thus, by investigating HDO rather than H₂O, we simplify the dynamics.

Surface charge density is an external parameter, which can modify the structure of interfacial water.⁵ The water/fused silica interface is an ideal model to explore the effect of surface charge on vibrational dynamics. Upon deprotonation of surface hydroxyl groups, the surface charge density at the silica/water interface generates an electric field, which consequently polarizes several layers of water molecules into the bulk and also appears to introduce more ordering in the structure of interfacial water.⁵

In the present study, using steady-state and time-resolved SFG, we probe the vibrational dynamics of the O–H stretching mode in the hydrogen-bonded region at the HDO:D₂O/silica interface at low and high bulk pH. In contrast to the H₂O/silica system where two peaks were observed in the SFG spectra,⁵ we report a single peak whose frequency red-shifts upon increasing the bulk pH in the SFG spectra of the HDO/silica interface. From the IR pump–SFG probe measurements, the vibrational lifetime of the OH stretch at the HDO/silica interface is observed to be frequency dependent with faster relaxation at the red as compared to the blue side of the hydrogen-bonded spectral region. At the charged surface, the measured dynamics is faster than in bulk water. On the contrary, at neutral pH, the interfacial vibrational dynamics is slower than in the bulk.

2. Experimental Section

2.1. Optical Table Setup. Approximately 90% of the output of a femtosecond regenerative amplifier (Quantronix, Integra-E; central wavelength 810 nm, repetition rate 1 kHz, pulsewidth \sim 110 fs fwhm, pulse energy \sim 3 mJ) is used to pump an optical parametric amplifier (Light Conversion, TOPAS), which generates tunable IR radiation (1180–2640 nm). Midinfrared pulses, \sim 170 cm⁻¹ fwhm, were obtained by difference frequency generation in an AgGaS₂ crystal with typical pulse energies of 20 μ J at 3 μ m. The mid-IR energy was divided, using a silicon wedge, to produce the pump and probe IR pulses with the ratio of 4:1. The remaining 10% of the regenerative amplifier output was used as the visible light for SFG measurements. The energy and polarization of the visible beam were adjusted by a combination of a half-wave plate and a prism polarizer. The IR pump, IR probe, and visible beams with energies of \sim 8, 2, and 2 μ J/pulse, incident at the surface with angles of

72°, 58°, and 65°, were focused to beam waists of 250, 200, and 200 μ m, respectively. The position of the zero time delay was determined by the third-order cross-correlation between IR pump, IR probe, and visible. The SFG signal was separated from the reflected visible light by short pass filters (Melles Griot) and was detected by a CCD detector (Princeton Instruments) coupled with a spectrograph (300i, Acton Research Corp.). A prism polarizer was used to select the detected polarization component of the SFG signal. In the experiments reported here, the SFG, visible, and IR beams were p-polarized.

2.2. Steady-State SFG Spectroscopy (VSFG Measurements). For steady-state vibrational SFG (VSFG) measurement, the visible pulse was spectrally narrowed to a fwhm of \sim 1.7 nm (25 cm⁻¹) by a pair of band-pass filters (CVI), and the IR probe was blocked. Because of the limited bandwidth of the IR pulse (\sim 170 cm⁻¹), a hybrid tuning-scanning broadband SFG approach²¹ was used to access the entire spectral region of the O–H stretching of water. Briefly, eight broadband SFG spectra with different IR input frequencies centered at 3000, 3100, 3200, 3300, 3400, 3500, 3600, and 3700 cm⁻¹ were acquired for the sample and reference. The sample and reference were a H₂O:HDO:D₂O mixture in contact with an infrared grade fused silica prism and a gold coated infrared fused silica prism, respectively. Each broadband SFG spectrum of the sample was normalized to the corresponding reference spectrum, and then all of the normalized spectra were summed together. To minimize spurious noise at the high and low frequency extremes of each of the spectra, essentially due to division by zero in the normalization, the intensity of reference SFG spectra was offset before normalization.^{21,22}

2.3. Time-Resolved SFG (IR Pump–SFG Probe). Time-resolved SFG (tr-SFG) experiments were performed in a one-color scheme in which an IR pulse (IR pump) with center frequency of ω ($\omega = 3200, 3300, \text{ or } 3450 \text{ cm}^{-1}$) transfers population from the ground to the first excited state. A combination of a second IR (IR probe) pulse, whose frequency and polarization are the same as in the IR pump, and a visible pulse generates a SFG signal, which monitors the ground-state population as a function of time. The third-order cross-correlation between IR pump, IR probe, and visible was used to maximize the SFG signal and to define the position of $t = 0$. The time delay between the IR probe and the visible was fixed, and the time delay between the IR pump and the IR probe (and visible) was scanned for tr-SFG and third-order cross-correlation measurements. The SFG was recorded in 50 fs time steps using LABVIEW software.

2.4. Sample Preparation. All glassware and the IR fused silica prism (ISP optics) and Teflon sample holder were cleaned by piranha solution (3:1 (v/v), concentrated sulfuric acid and 30% hydrogen peroxide) prior to experiments. Solutions were prepared using HCl (Fisher, ACS Certified), NaOH (Fisher, ACS certified), NaCl (Fisher, ACS certified), and D₂O (Cambridge Isotope Laboratories, Inc., purity 99.9%) and distilled Millipore water ($>18.2 \text{ M}\Omega \text{ cm}$ resistivity). To reduce the contribution from H₂O, the initial percentage of H₂O and D₂O was chosen to be 15% and 85%, respectively, which gives a final composition of H₂O:HDO:D₂O: 1:11:32. All of the pH solutions were prepared at the constant ionic strength by adding NaCl. To remove impurities, the as-received NaCl was heated at \sim 550 °C overnight.²³

3. Results and Discussion

The ratio of H₂O:HDO:D₂O in the experiment reported here was 1:11:32. HDO was sufficiently dilute to reduce the

- (14) Kropman, M. F.; Nienhuys, H. K.; Woutersen, S.; Bakker, H. J. *J. Phys. Chem. A* **2001**, *105*, 4622–4626.
- (15) Corcelli, S. A.; Skinner, J. L. *J. Phys. Chem. A* **2005**, *109*, 6154–6165.
- (16) Woutersen, S.; Emmerichs, U.; Bakker, H. J. *Science* **1997**, *278*, 658–660.
- (17) Rey, R.; Hynes, J. T. *J. Chem. Phys.* **1996**, *104*, 2356–2368.
- (18) Tian, C.; Shen, Y. R. *J. Am. Chem. Soc.* **2009**, *131*, 2790–2791.
- (19) Sovago, M.; Campen, R. K.; Wurpel, G. W. H.; Muller, M.; Bakker, H. J.; Bonn, M. *Phys. Rev. Lett.* **2008**, *100*.
- (20) Raymond, E. A.; Tarbuck, T. L.; Richmond, G. L. *J. Phys. Chem. B* **2002**, *106*, 2817–2820.

- (21) Voges, A. B.; Stokes, G. Y.; Gibbs-Davis, J. M.; Lettan, R. B.; Bertin, P. A.; Pike, R. C.; Nguyen, S. T.; Scheidt, K. A.; Geiger, F. M. *J. Phys. Chem. C* **2007**, *111*, 1567–1578.
- (22) Ma, G.; Chen, X. K.; Allen, H. C. *J. Am. Chem. Soc.* **2007**, *129*, 14053–14057.
- (23) Bian, H. T.; Feng, R. R.; Xu, Y. Y.; Guo, Y.; Wang, H. F. *Phys. Chem. Chem. Phys.* **2008**, *10*, 4920–4931.

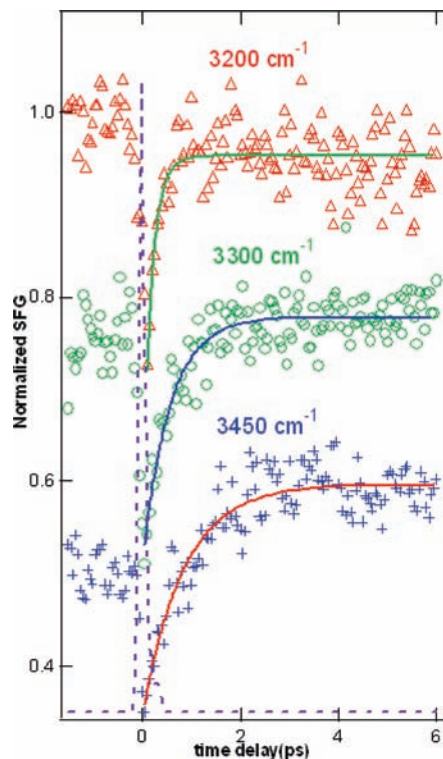


Figure 1. IR pump–SFG probe vibrational dynamics of the O–H stretch at the HDO/silica interface at pH = 12 with different pump (and probe) frequencies. The solid line is the single exponential fit consistent with a three-level system. The third-order cross-correlation between IR pump, IR probe, and visible is shown by the dashed line.

intermolecular energy transfer rate and yet provide sufficient signal to be able to investigate the interfacial vibrational spectroscopy and dynamics. The order of magnitude higher concentration of HDO as compared to H₂O, and the fact that the SFG signal is proportional to the square of the molecular density, ensures that the SFG signal in the O–H stretching region predominantly comes from the HDO species and that the contribution of H₂O is negligible. With this understanding, we write HDO/silica interface, instead of H₂O:HDO:D₂O/silica interface, throughout this Article.

The results of IR pump–SFG probe of O–H stretching vibrational dynamics at the HDO/silica interface at pH = 12 and pH = 2 with pumping at three different frequencies centered at 3200, 3300, and 3450 cm⁻¹ are shown in Figures 1 and 2. A three-level system and therefore a single time constant describing the vibrational lifetime (*T*₁) are sufficient to capture the dynamics. A similar analysis was used to describe the intramolecular relaxation of bulk dilute HDO in D₂O²⁴ and of membrane bound water.²⁵

In both the 3200 and the 3450 cm⁻¹ regions, the SFG signal does not recover to its initial value in the time scales explored in these experiments. This offset is attributed to the temperature jump resulting from the dissipation of excess energy to the hydrogen-bond network and has been observed in previous surface and bulk studies of vibrational dynamics of water.^{14,25} The instantaneous temperature jump, which is estimated to be less than 5 K (neglecting heat diffusion out of the excited

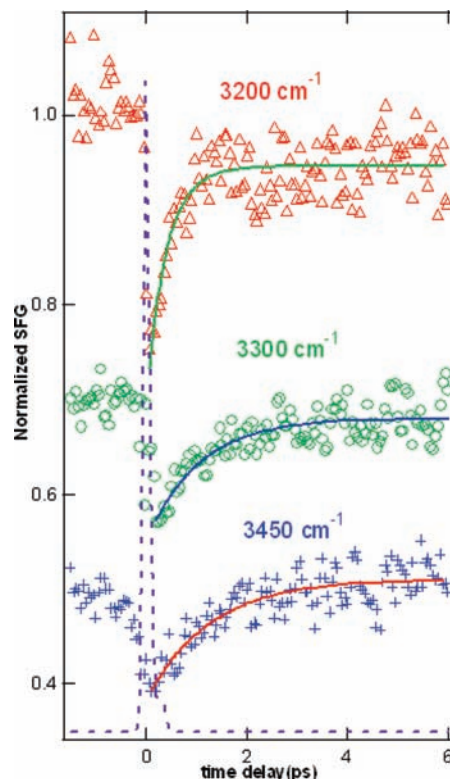


Figure 2. IR pump–SFG probe vibrational dynamics of the O–H stretch at the HDO/silica interface at pH = 2 with different pump (and probe) frequencies. The solid line is the single exponential fit consistent with a three-level system. The third-order cross-correlation between IR pump, IR probe, and visible is shown by the dashed line.

volume on the picosecond time scale) in our setup, leads to a weakening of the hydrogen-bond network and therefore a decrease/increase in the relative density of water molecules with strong/weak hydrogen bonds. Because the number of water molecules with a stronger hydrogen-bond network is higher at 3200 than at 3450 cm⁻¹, the SFG signal at long time delays (2–6 ps) is lower/higher than its initial values at 3200/3450 cm⁻¹ region, respectively. At 3300 cm⁻¹, because the excitation (and probe) wavelengths are between the region with more/less hydrogen-bond network, the offset is not significant.

The O–H vibrational dynamics of the HDO/silica interface show remarkable frequency dependence. Frequency-dependent vibrational lifetimes were also observed for 0.5% bulk solution of HDO in D₂O.²⁶ The *T*₁ decreased from 1 ps at ~3600 cm⁻¹ to <0.5 ps at 3270 cm⁻¹ and was explained by intramolecular energy transfer between the excited state O–H and the overtone of the bending mode of HDO (~2900 cm⁻¹).²⁶ Recent molecular dynamics simulations also predict the frequency dependence of bulk vibrational lifetimes based on energy-gap-law considerations²⁷ where the determining factor for the rate of vibrational relaxation is the energy gap between the excited state and the intermediate state energy levels. The smaller the energy gap between these two states, the shorter the vibrational lifetime will be. The intermediate state can be the hydrogen-bond stretch or the overtone of the bending mode. We consider both possibilities.

(24) Lock, A. J.; Woutersen, S.; Bakker, H. J. *J. Phys. Chem. A* **2001**, *105*, 1238–1243.

(25) Ghosh, A.; Smits, M.; Bredenbeck, J.; Bonn, M. *J. Am. Chem. Soc.* **2007**, *129*, 9608+.

(26) Gale, G. M.; Gallot, G.; Lascoux, N. *Chem. Phys. Lett.* **1999**, *311*, 123–125.

(27) Lawrence, C. P.; Skinner, J. L. *J. Chem. Phys.* **2003**, *119*, 3840–3848.

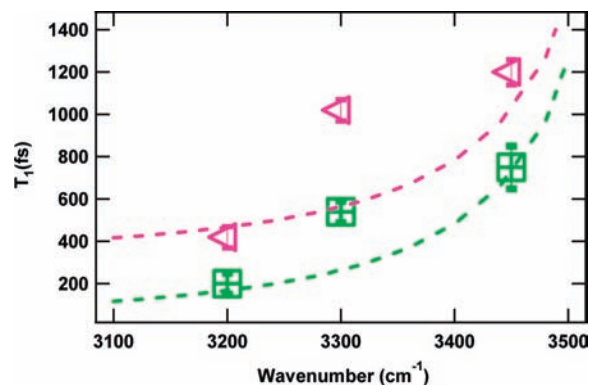


Figure 3. Frequency-dependent vibrational lifetime (T_1) of the O–H stretch at the HDO/silica interface at pH = 2 (purple triangle) and pH = 12 (green square). The dashed lines are the theoretical model that describes the frequency dependence of T_1 . The errors bars are estimated from the average of more than two data sets from independent experiments.

If the hydrogen-bond stretch (O–H \cdots O) is the accepting mode, the theoretical model of Hynes et al. predicts that the dependence of the vibrational lifetime (T_1) on the strength of the hydrogen bond is proportional to $(\delta\omega)^{-1.8}$ where $\delta\omega = \omega(\text{free OH}) - \omega(\text{hydrogen-bonded OH})$.²⁸ The variation of the vibrational lifetime as a function of the IR excitation frequency for both pH = 12 and pH = 2 is plotted in Figure 3. It is clear that the experimental vibrational lifetime at both pH values is well described by the theoretical model (dotted line). At 3300 cm^{-1} , however, there is a deviation of the experimental value of T_1 from the predicted theory. This deviation can be accounted for by noting that, due to the 170 cm^{-1} bandwidth of the IR pulse, when exciting at 3300 cm^{-1} there is a contribution from the blue ($>3300 \text{ cm}^{-1}$) and red ($<3300 \text{ cm}^{-1}$) side, which causes the T_1 to have a larger value than the theoretical model predicts. If, on the other hand, the overtone of the bending mode is considered as the intermediate accepting mode, the energy gap difference between the excited state O–H stretch and the first overtone of the HDO bend (2900 cm^{-1}) is smaller when pumping at lower frequency (3200 cm^{-1}) than higher frequency (3450 cm^{-1}). The smaller energy gap between the two states then facilitates energy relaxation, consistent with the faster relaxation at 3200 cm^{-1} as compared to 3450 cm^{-1} .

Predicting the exact channel for vibrational energy transfer is not straightforward as illustrated in the case of the bulk dynamics studies of HDO:D₂O. Kropman et al.¹⁴ suggested the hydrogen-bond stretch modes as the main accepting mode, with smaller contributions from the bending mode. On the other hand, Deak et al.¹³ proposed the bending mode of HDO as the dominant channel for the energy relaxation of the excited O–H stretch, although some of the energy can relax via hydrogen-bond modes. Yet another view is provided by the experimental study of HDO:D₂O by Gale et al.²⁶ and the theoretical models by Skinner group²⁷ that have suggested the overtone of the bending mode as the important channel for the vibrational energy transfer of the excited state O–H. We show that the observed dynamics can be explained by both the Hynes model²⁸ (with the hydrogen-bond stretch as the main channel for accepting the vibrational energy) and the energy gap law (with the overtone of the bending as the main channel for accepting the vibrational energy). As the dynamics is consistent with both models, we cannot distinguish whether the hydrogen-bond

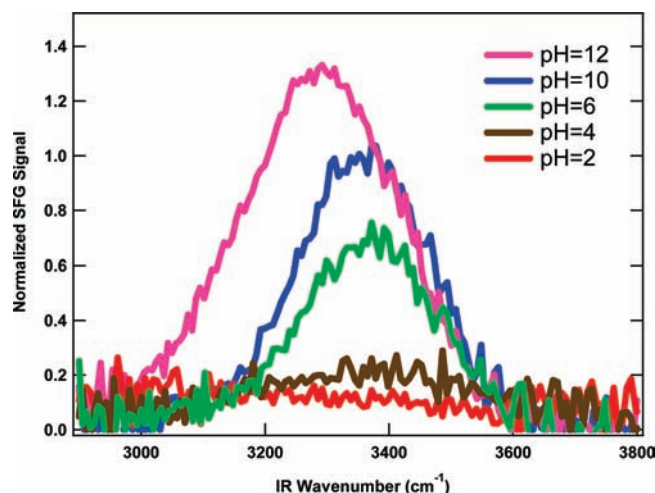


Figure 4. VSFG spectra of the HDO/silica interface at different pH values and constant ionic strength (the ratio of H₂O:HDO:D₂O is 1:11:32).

stretch or the overtone of the bending is the main accepting mode, or even if both play a significant role.

Comparing the vibrational lifetime at different pH values, it is apparent that the vibrational lifetime at a given IR frequency is faster at pH = 12 than at pH = 2. To explain the dynamics, the VSFG spectra of the HDO/silica interface at different pH were measured (Figure 4). Similar to the VSFG of the H₂O/silica interface,⁵ the VSFG intensity increases with increasing bulk pH. However, in contrast to VSFG of the H₂O/silica interface where two peaks were observed,⁵ a single peak is observed in the VSFG of the HDO/silica interface (Figure 4). Furthermore, unlike the H₂O/silica interface, where the peak positions remained unchanged with changing pH, increasing the pH results in the red-shift of the peak in the VSFG of the HDO/silica interface. The increase in the intensity and the red-shift of the peak in the VSFG spectra suggest an increasingly ordered structure of interfacial water with a more developed and stronger hydrogen-bond network that is induced by the electric field resulting from the surface charge at high pH.

Given the small VSFG intensity at pH = 2 as compared to pH = 12, one may argue that the pump–probe response at pH = 2 could be due to the nonresonant response. We repeated the VSFG spectra at pH = 2 and pH = 4 more than two times, and in all cases we observed very small VSFG signals at pH = 2 and pH = 4 as compared to higher pH. We also acquired the VSFG spectra of H₂O/silica at different pH values (data are not shown). The overall features of the spectra (increase in the VSFG intensity as pH increases, appearance of two peaks at ~ 3200 and 3400 cm^{-1} with no peak shift with change in pH) were similar to the previous reported VSFG of H₂O/silica.^{29–32} However, even in the case of H₂O/silica, the VSFG at pH = 2 was very small as compared to higher pH. In the pump–probe traces, the magnitude of the SFG signal before excitation (at negative time delay where the pump arrives at the sample after the probe) is a factor of ~ 4 smaller at pH = 2 as compared to pH = 12. To test the possibility of a nonresonant contribution

(28) Staib, A.; Hynes, J. T. *Chem. Phys. Lett.* **1993**, *204*, 197–205.

(29) Du, Q.; Freysz, E.; Shen, Y. R. *Phys. Rev. Lett.* **1994**, *72*, 238–241.

(30) Kim, J.; Kim, G.; Cremer, P. S. *J. Am. Chem. Soc.* **2002**, *124*, 8751–8756.

(31) Nihonyanagi, S.; Ye, S.; Uosaki, K. *Electrochim. Acta* **2001**, *46*, 3057–3061.

(32) Ostroverkhov, V.; Waychunas, G. A.; Shen, Y. R. *Chem. Phys. Lett.* **2004**, *386*, 144–148.

in the time-resolved experiment, the IR pump–SFG probe response of the silica/D₂O system was measured at 3200 cm⁻¹, and there was no observed bleach at pH = 2 or 12 (data are not shown).

The static electric field at high pH penetrates into the bulk water and extends the anisotropic interfacial regions into the initially centrosymmetric bulk phase, which results in the contribution of the third-order nonlinear susceptibility ($\chi^{(3)}$) to the SFG, in addition to the second-order term ($\chi^{(2)}$).³³ As a result, the number of water molecules contributing to the VSFG increases, enhancing the intensity of the VSFG. The electric field (E_{DC}) orients some of the water via the molecular dipole moment (μ), basically those species for which $\mu \cdot E_{DC} > kT$, resulting in a more ordering environment for the near interface species. This is reflected in the red-shift of the VSFG peak as the pH, and interfacial electric field, increases. The red-shift in the vibrational spectrum of water is associated with increased H bonding.³⁴ The contribution of these ordered water molecules to the faster dynamics at pH = 12 can be justified by the theoretical model of Hynes described above. According to the Hynes model, the further the frequency of O–H of hydrogen-bonded water molecules is from the free OH, the shorter is the vibrational lifetime.²⁸ The VSFG spectra of the HDO/silica interface at different pH values (Figure 4) show a substantial red-shift of frequency of O–H with increasing pH. This red-shift can partially explain the faster dynamics at high pH as $T_1 \propto (\delta\omega)^{-1.8}$.

In addition to the ordering effect, due to the penetration of electric field into the bulk water, the SFG probes water molecules that may in principle be as far as the Debye length from the interface, resulting in dynamics that is similar to bulk water. The contribution of these polarized water (which are not necessarily ordered) to the faster dynamics at pH = 12 can be explained by the hypothesis that these polarized water molecules are completely solvated. In contrast, when the surface charge is zero, SFG principally probes water molecules in the first layer at the interface. These molecules have lost part of their solvation shell, leading to a decrease in the number of intermolecular accepting modes for the vibrational energy. The consequence is less efficient inter- and intramolecular coupling and ultimately an increase in the vibrational lifetime. It is noted that, although the major step in the vibrational relaxation, from the excited state to the intermediate state, proceeds via intramolecular energy transfer, intermolecular modes are vital to make up the energy gap between the accepting mode and the excited state O–H.

Another interesting observation is that, although at high pH SFG probes the dynamics of bulk-like water, the value of T_1 is shorter for interfacial HDO at pH = 12 than for bulk HDO. The shorter T_1 of the interfacial HDO at high pH is most likely the result of the increased ordering/hydrogen bonding of interfacial water at the charged surface, as revealed by the SFG spectra (Figure 4). It is known from the temperature dependence dynamics of bulk HDO that the dynamics of more ordered HDO ice is faster than disordered HDO liquid.³⁵ Observing the effect of ordering on the vibrational dynamics of interfacial water at high pH would not be possible in pure H₂O because of rapid

resonant energy transfer, which is significantly reduced in diluted HDO. It is noted that, according to bulk dynamics studies of HDO in D₂O, at a concentration of HDO (~10 M) similar to the present measurements, there still remains some contribution of intermolecular energy transfer to the dynamics.^{12,13} However, as compared to bulk water, the intermolecular energy transfer is expected to be less efficient at the interface as water molecules have a lower density of neighbors to transfer energy to. Nevertheless, even with some contribution of intermolecular energy transfer, the overall picture remains the same; the slower rate of intermolecular energy transfer in HDO as compared to H₂O helps to resolve the spectral diffusion in the dynamics of HDO:D₂O at the silica interface.

The slowing of the vibrational dynamics at low pH observed here is analogous with the behavior of water confined in reversed micelles where the water molecules in the vicinity of the surfactant have longer vibrational dynamics than water molecules in the core shell (which display bulk water response).^{36,37} Similarly, simulations of the vibrational dynamics of solutes at aqueous interfaces predict a lengthening of the vibrational lifetime as compared to the bulk. The longer vibrational lifetime of solutes (more significant for neutral than charged solutes) was attributed to the reduced of solvent number density (nearest neighbor molecules) as compared to the bulk and the ability of solutes to hold their hydration shell at the interface.

The vibrational lifetimes observed here (Figure 3) are significantly longer than those reported previously for pure H₂O at the water/silica interface at pH = 5.7 (~300 fs),¹⁰ the H₂O/silica at pH = 2 (570 fs) and pH = 12 (255 fs),¹¹ the air/water interface (~100 fs),⁸ and the membrane–water interface (100–570 fs).²⁵ The behavior of dilute HDO at the silica/water interface is similar to the vibrational dynamics of dilute bulk HDO where the vibrational lifetime of the O–H stretching of HDO:D₂O (740 fs) was more than 3 times slower than that of O–H of pure H₂O (~200 fs).^{14,24} We attribute the increase of the vibrational lifetime of O–H of HDO, as compared to O–H of H₂O, to the energy-gap-law argument. For H₂O, the overtone of the bending mode is centered at ~3280 cm⁻¹. The energy gap difference between the first excited state O–H stretch and the first overtone of the bending mode is ~±100 cm⁻¹ for pumping at either 3200 or 3400 cm⁻¹; that is, the difference between these excitation wavenumbers and the overtone of the bending mode is the same for H₂O. Hence, no frequency-dependent vibrational lifetime was observed for the H₂O/silica interface^{10,11} or the H₂O/air interface.⁸ For HDO, however, the overtone of the bending mode is ~2900 cm⁻¹. The energy gap between the O–H stretch and the bending overtone is then ~300–500 cm⁻¹ (depending on whether pumping occurs at 3200 or 3450 cm⁻¹). The larger energy gap in the case of HDO can partially explain the longer vibrational lifetime. It is noted that in the dynamics of bulk water the frequency-dependent T_1 was found to be the result of the contribution of the hydrogen-bond breaking to the observed vibrational excited state dynamics.³⁸ By decomposing the transient vibrational spectra of the HDO:D₂O system into two components associated with vibrational excited state lifetime and the effect of hydrogen-bond breaking on the vibrational excited state, a frequency-indepen-

(33) Ong, S. W.; Zhao, X. L.; Eisenhal, K. B. *Chem. Phys. Lett.* **1992**, *191*, 327–335.

(34) Sovago, M.; Campen, R. K.; Bakker, H. J.; Bonn, M. *Chem. Phys. Lett.* **2009**, *470*, 7–12.

(35) Woutersen, S.; Emmerichs, U.; Nienhuys, H. K.; Bakker, H. J. *Phys. Rev. Lett.* **1998**, *81*, 1106–1109.

(36) Park, S.; Moilanen, D. E.; Fayer, M. D. *J. Phys. Chem. B* **2008**, *112*, 5279–5290.

(37) Cringus, D.; Lindner, J.; Milder, M. T. W.; Pshenichnikov, M. S.; Vohringer, P.; Wiersma, D. A. *Chem. Phys. Lett.* **2005**, *408*, 162–168.

(38) Steinel, T.; Asbury, J. B.; Zheng, J. R.; Fayer, M. D. *J. Phys. Chem. A* **2004**, *108*, 10957–10964.

dent vibrational lifetime of the O–D stretch was observed.³⁸ Although hydrogen-bond breaking may contribute to the frequency-dependent T_1 observed here, more experimental and theoretical studies would be required to make a definitive statement.

4. Conclusion

It is apparent that a wealth of information on the details of the local environment of the hydrogen-bond network of interfacial water can be obtained by studying dilute solutions of HDO in D₂O. Frequency-dependent dynamics, and the change in the O–H frequency with changing pH, suggest that the O–H stretching of HDO is an excellent probe of the local hydrogen-bond environment. Such information is hidden in the spectroscopy and dynamics of pure H₂O due to the intramolecular

coupling between the O–H of individual H₂O and intermolecular coupling with its neighbors.

The dynamics observed here is in stark contrast with the previous studies of interfacial vibrational dynamics of water, which concluded that the vibrational dynamics of bulk and interfacial water are similar. It is now clear that the structural differences between the surface and the bulk result in noticeably different vibrational dynamics. Our results shed light on, and open a new window for, the characterization of interfacial water especially when an external field modifies the interfacial structure.

Acknowledgment. This research was supported by the ACS-PRF.

JA907745R